

Concerted Hydrogen-Bond Breaking by Quantum Tunneling in the Water Hexamer Prism

Jeremy O. Richardson,^{1,2*} Cristóbal Pérez,^{3†} Simon Lobsiger,³
Adam A. Reid,^{1‡} Berhane Temelso,⁴ George C. Shields,⁴
Zbigniew Kisiel,⁵ David J. Wales,¹ Brooks H. Pate,^{3*} Stuart C. Althorpe^{1*}

¹Department of Chemistry, University of Cambridge, Lensfield Road, Cambridge,
CB2 1EW, United Kingdom

²Department of Chemistry, Durham University, South Road, Durham,
DH1 3LE, United Kingdom

³Department of Chemistry, University of Virginia, McCormick Road,
Charlottesville, VA 22903, USA

⁴Dean's Office, College of Arts and Sciences, and Department of Chemistry,
Bucknell University, Lewisburg, PA 17837, USA

⁵Institute of Physics, Polish Academy of Sciences, Al. Lotników 32/46,
02-668 Warszawa, Poland

*To whom correspondence should be addressed.

E-mail: jeremy.richardson@durham.ac.uk (JOR);
brookspate@virginia.edu (BHP); sca10@cam.ac.uk (SCA)

†Current address: Max Planck Institute for the Structure and Dynamics of Matter,
Luruper Chausse 149, D-22761 Hamburg, Germany

‡Current address: Department of Mathematics, Tonbridge School, High St,
Tonbridge, TN9 1JP, United Kingdom

The nature of the intermolecular forces between water molecules is the same in small hydrogen-bonded clusters as in the bulk. The rotational spectra of the clusters therefore give insight into the intermolecular forces present in liquid

water and ice. The water hexamer is the smallest water cluster to support low-energy structures with branched three-dimensional hydrogen-bond networks, rather than cyclic two-dimensional topologies. Here we report measurements of splitting patterns in rotational transitions of the water hexamer prism, and use quantum simulations to show that they result from geared and anti-geared rotations of a pair of water monomers. Unlike previously reported tunneling motions in water clusters, the geared motion involves the concerted breaking of two hydrogen bonds. Similar types of motion may be feasible in interfacial and confined water.

In addition to its bulk phases, water can form small gas-phase clusters $(\text{H}_2\text{O})_n$, in which the molecules are held together by a network of hydrogen bonds. The cluster dynamics can be probed by high-resolution rovibrational spectroscopy (1–9) and interpreted by theoretical simulations (10–27). The nature of the interactions between the water molecules is the same in the clusters as in the bulk (many-body forces beyond the three-body term are relatively weak) (28), and hence the cluster spectra can be used to test universal models (25, 29–32) of the water intermolecular potential energy surface, giving insight into hydrogen bonding in all phases of water. At low temperatures, the molecules are frozen into a network and can only rearrange by quantum tunneling, which causes splittings in the spectrum ranging from MHz to THz (33). Quantum simulations (10–27) have identified rearrangements which involve free hydrogen flips that break no hydrogen bonds, and bifurcations that break one bond (2).

Here, we report observation of a tunneling motion that concertedly breaks two hydrogen bonds in a water cluster. The hexamer is the smallest cluster with a branched three-dimensional equilibrium geometry (5) and has thus been dubbed the smallest droplet of water. It has a variety of isomers (12–14, 21, 34–36), of which the spectrum of the lowest energy prism isomer, PR1 of Fig. 1 (see the supplementary materials for a discussion of other prism isomers) was recently

found to show a splitting pattern, which was attributed to tunneling (6). Here we report new measurements and quantum simulations on PR1 which uncover the dynamics responsible for the splittings.

Tunneling in water clusters occurs when the molecules in their equilibrium geometry rearrange to produce an equivalent structure, by permuting equivalent atoms, or inverting the structure through its center-of-mass. These geometrically identical structures (which can be distinguished only by labeling the atoms and specifying the chirality) are termed versions. The number of versions is equal to the size of the group of all nuclear permutations and inversions (37), which for PR1 gives an enormous total of $2 \times 6! \times 12! \simeq 10^{12}$. However, only versions linked by short and energetically accessible tunneling pathways produce observable splittings. We therefore need to consider only pathways that rotate the water molecules within the structure, as these avoid breaking covalent bonds. For smaller clusters, these rules are sufficient to assign tunneling splittings (2, 15, 16, 20, 27). However, for PR1, the size of the space left to explore is still vast.

To narrow down further the number of likely tunneling pathways, we measured the rotational spectra of all 64 isotopologues of the hexamer PR1 prism with formula $(\text{H}_2^{18}\text{O})_n(\text{H}_2^{16}\text{O})_{6-n}$ ($n = 0 \dots 6$); these are presented in Tables S5–68. Figure 2a shows the tunneling patterns for three *a*-type rotational transitions of the $(\text{H}_2^{16}\text{O})_6$ cluster. These spectra show the characteristic splitting pattern previously observed (6). Isotopic substitution destroys this pattern, except in $(\text{H}_2^{18}\text{O})_6$ and in the six doubly-substituted isotopologues shown in Fig. 2b. This tells us immediately that the tunneling paths must rearrange two separate water molecules in the structure, ruling out motions such as the flip and bifurcation observed in other water clusters (2, 15, 16, 20, 27). Closer inspection shows that the observed splitting is slightly reduced when the A+D dimer is substituted with the heavier isotope; the composition of the remaining tetramer portion of the cluster does not affect the splitting. The tunneling motion must therefore

involve rearrangements of molecules A and D, and the dynamics are probably localized in this part of the cluster.

To elucidate the dynamics further it was necessary to carry out quantum simulations on an accurate potential energy surface. Full quantum calculations are impossible for this 48-degree-of-freedom problem, and so we used the ring-polymer instanton (RPI) method (27, 38). This method assumes that the tunneling can be approximated by fluctuations around the minimum-action or instanton paths connecting different versions. The instanton path is found by minimizing the potential energy of a fictitious polymer formed by linking replicas of the system by harmonic springs. Previous studies on other water clusters (27, 39) have shown that this method correctly predicts the pattern and order-of-magnitude of the tunneling splittings, and that the instanton paths give a useful representation of the tunneling dynamics. Further details of the RPI method are given in the supplementary materials. The potential energy surface used was the HBB2-pol surface (31); we also made comparisons with the MB-pol surface (32), and found no major qualitative differences in the results (Table S1).

Because the space of possible tunneling paths is vast, it is necessary to have an idea of the starting path, which can then be refined using the RPI method. Initially, we considered paths that resemble the flip motions observed in other water clusters, which involve the wag of a non-hydrogen-bonded H-atom. No single flip connects versions in the hexamer prism but a double-flip corresponding to the permutation $P_a = (A\ D)(B\ F)(C\ E)(1\ 7)(2\ 8)(3\ 11)(4\ 12)(5\ 9)(6\ 10)$ (using the labeling in Fig. 1) does. The resulting instanton path is shown in Fig. 3a (and the corresponding transition-state in Fig. S1a). Unlike single flips, this double-flip breaks one hydrogen bond. We call this the anti-gear path because the H-1 rotates out of its hydrogen bond in the opposite sense to H-7 (which rotates in to form a hydrogen bond with O-A).

Because $P_a^2 = E$ (the identity), it follows that the anti-gear path gives a simple doublet splitting pattern. Now, P_a is the only permutation that breaks no more than one hydrogen bond.

Hence the observed pattern (Fig. 2a), in which the doublet is split further into six lines, implies that, unlike other water clusters, the PR1 hexamer supports tunneling paths that break two or more hydrogen bonds. In other water clusters, the next most feasible tunneling pathways after the flips are bifurcations, in which an H-atom rotates away from its hydrogen bond and is replaced by the other H-atom on the same water molecule (15). This mechanism breaks only one hydrogen bond in the trimer, but in PR1, owing to its three-dimensional structure, such a bifurcation rearrangement must break at least two hydrogen bonds. We located a variety of single-bifurcation tunneling pathways, but found that, as in the water octamer (39), the resulting instanton tunneling splittings were tiny, indicating that these paths are unfeasible. However, we found that there exists a single feasible pathway that combines a double-flip with a bifurcation, corresponding to the permutation $P_g = (A D)(B F)(C E)(1 8 2 7)(3 11)(4 12)(5 9)(6 10)$. This path also breaks two hydrogen bonds, but surprisingly, the resulting instanton pathway (Fig. 3b) gives a small but observable tunneling splitting. This is because it describes a geared pathway, in which atoms H-1 and H-7 rotate in the same sense, resulting in a reduction in energy which offsets the increase in energy required to break the additional H-2...O-B hydrogen bond.

The combination of both the geared and anti-geared pathways explains the doublet-of-triplets splitting observed in the spectrum. P_a and P_g generate a group of permutations (described in the supplementary materials) which link together eight versions of the prism; Fig. 4a shows the graph which represents the connections between versions associated with these two tunneling pathways. To predict the splitting pattern, we must first obtain the energy levels by diagonalizing the tunneling matrix \mathbf{h} (Fig. 4b), in which every connection in the graph is represented by a matrix element h_{ij} (where $i, j = 1, \dots, 8$ label the versions). These elements were calculated using a normal-mode analysis of the ring-polymer instantons (27, 38). Elements corresponding to a direct link by a single instanton path gave the values $h_a = -0.88$ MHz (anti-geared) and $h_g = -0.15$ MHz (geared); all other permutations in the group were found

to give negligibly small values of h_{ij} , which were thus set to zero. The resulting energy-level splitting obtained by diagonalizing the tunneling matrix is given in Fig. 4c. A symmetry analysis of the non-rigid cluster (37) shows that the eigenfunctions of the tunneling matrix transform as irreducible representations of a group isomorphic to the D_{2d} point group. We can therefore assign symmetry labels to the levels (Fig. 4).

In the hexamer prism, the energy level splittings caused by tunneling (order of MHz) are significantly smaller than the energy separation for the rotational energy levels (several GHz). Therefore, it is appropriate to consider a tunneling energy level pattern for each different rotational level—these patterns can have a slight dependence on the rotational quantum numbers as suggested by Fig. 2a. To obtain the splitting pattern in the rotational spectrum which consists of transitions between the tunneling states for different rotational levels, we note that μ_a transforms as B_2 and only allows strong transitions between the tunneling states $A_1 \leftrightarrow B_2$, $A_2 \leftrightarrow B_1$ and $E_{(1)} \leftrightarrow E_{(2)}$. These transitions give the doublet-of-triplet splitting pattern shown in Fig. 4c and the amplitudes of the pattern are obtained from the nuclear-spin statistics. As explained in the supplementary materials, there are also some pure rotational transitions which are not rigorously forbidden by symmetry but contribute only weakly to a small central peak, and evidence of these nominally forbidden transitions appears in Fig. 2. As shown in Fig. 4d, the theoretical splitting pattern qualitatively reproduces the experimentally observed splitting pattern, but is about twice as wide. An analysis of the J -dependent geared and anti-geared tunneling matrix elements, presented in the supplementary materials, gives the values of $h_a = -0.382$ MHz and $h_g = -0.073$ MHz for the ground state, which can be compared directly to the theoretical values given above. The ratio of the theoretical matrix elements $h_g : h_a$ is 1 : 5.8 and in excellent agreement with the experimental value of 1 : 5.2. Furthermore, full isotopic substitution of ^{16}O with ^{18}O is found to reduce the predicted tunneling matrix elements to 85% of their value, indicating a slight participation of the heavy oxygen-atom framework during tunneling. This

is confirmed by the experimental tunneling splittings (Fig. 2b), which are proportional to the tunneling matrix elements, where the observed reduction is 84%. This level of agreement is good for an instanton calculation and is consistent with previous applications to other water clusters (27, 39), where the main errors in the instanton calculation were attributed to neglect of anharmonicity in the fluctuations around the instanton, along with rotation-tunneling coupling. This implies that the potential energy surfaces give an excellent description of the intermolecular force and we can be confident that the geared and anti-geared tunneling pathways in Fig. 3 correctly describe the tunneling responsible for the observed splittings.

Plots of the potential energy along the tunneling paths (Fig. 3) show striking differences between the instanton and minimum-energy paths. The mass-weighted length of the minimum-energy path is four times that of the instanton path for the anti-geared pathway, and twice that for the geared. A naive one-dimensional analysis using the minimum-energy paths might conclude that the geared tunneling is more facile than the anti-geared (because the effective barrier is much thinner), and that in either case the splitting pattern is probably too small to be observed on account of the long tunneling pathways. That the splittings are observable and that the ratio is the other way round are the result of corner cutting by the instanton pathway (40). Unlike the minimum-energy path, it bypasses the transition state in order to avoid the penalty in the action associated with moving the heavy oxygen atoms.

It is likely that other prism clusters, such as the pentagonal prism decamer, could exhibit similar pathways. These results also raise the possibility that the rearrangement dynamics of water in interfacial (41, 42) or confined environments might also involve similar concerted breaking of two (or more) hydrogen bonds.

References and Notes

1. A. C. Legon, D. J. Millen, *Chem. Soc. Rev.* **21**, 71 (1992).

2. N. Pugliano, R. J. Saykally, *Science* **257**, 1937 (1992).
3. R. J. Saykally, G. A. Blake, *Science* **259**, 12 (1993).
4. K. Liu, J. D. Cruzan, R. J. Saykally, *Science* **271**, 929 (1996).
5. F. N. Keutsch, R. J. Saykally, *P. Natl. Acad. Sci. USA* **98**, 10533 (2001).
6. C. Pérez, *et al.*, *Science* **336**, 897 (2012).
7. R. J. Saykally, D. J. Wales, *Science* **336**, 814 (2012).
8. C. Pérez, *et al.*, *Chem. Phys. Lett.* **571**, 1 (2013).
9. C. Pérez, *et al.*, *Angew. Chem. Int. Edit.* **53**, 14368 (2014).
10. S. C. Althorpe, D. C. Clary, *J. Chem. Phys.* **101**, 3603 (1994).
11. D. Sabo, Z. Bačić, T. Bürgi, S. Leutwyler, *Chem. Phys. Lett.* **244**, 283 (1995).
12. K. Liu, *et al.*, *Nature* **381**, 501 (1996).
13. K. Liu, M. G. Brown, R. J. Saykally, *J. Phys. Chem. A* **101**, 8995 (1997).
14. D. J. Wales, *Theory of Atomic and Molecular Clusters: With a Glimpse at Experiments*, J. Jellinek, ed. (Springer-Verlag, Berlin, 1999), pp. 86–110.
15. D. J. Wales, *J. Am. Chem. Soc.* **115**, 11180 (1993).
16. T. R. Walsh, D. J. Wales, *J. Chem. Soc. Faraday Trans.* **92**, 2505 (1996).
17. D. J. Wales, T. R. Walsh, *J. Chem. Phys.* **105**, 6957 (1996).
18. D. J. Wales, T. R. Walsh, *J. Chem. Phys.* **106**, 7193 (1997).

19. J. K. Gregory, D. C. Clary, *J. Chem. Phys.* **103**, 8924 (1995).
20. J. K. Gregory, D. C. Clary, *J. Chem. Phys.* **102**, 7817 (1995).
21. J. K. Gregory, D. C. Clary, *J. Phys. Chem. A* **101**, 6813 (1997).
22. E. H. T. Olthof, A. van der Avoird, P. E. S. Wormer, K. Liu, R. J. Saykally, *J. Chem. Phys.* **105**, 8051 (1996).
23. C. Leforestier, L. B. Braly, K. Liu, M. J. Elrod, R. J. Saykally, *J. Chem. Phys.* **106**, 8527 (1997).
24. R. S. Fellers, L. B. Braly, R. J. Saykally, C. Leforestier, *J. Chem. Phys.* **110**, 6306 (1999).
25. R. Bukowski, K. Szalewicz, G. C. Groenenboom, A. Van der Avoird, *Science* **315**, 1249 (2007).
26. X. Huang, *et al.*, *J. Chem. Phys.* **128**, 034312 (2008).
27. J. O. Richardson, S. C. Althorpe, D. J. Wales, *J. Chem. Phys.* **135**, 124109 (2011).
28. U. Góra, R. Podeszwa, W. Cencek, K. Szalewicz, *J. Chem. Phys.* **135**, 224102 (2011).
29. Y. Wang, B. C. Shepler, B. J. Braams, J. M. Bowman, *J. Chem. Phys.* **131**, 054511 (2009).
30. Y. Wang, X. Huang, B. C. Shepler, B. J. Braams, J. M. Bowman, *J. Chem. Phys.* **134**, 094509 (2011).
31. V. Babin, G. R. Medders, F. Paesani, *J. Phys. Chem. Lett.* **3**, 3765 (2012).
32. V. Babin, G. R. Medders, F. Paesani, *J. Chem. Theory Comput.* **10**, 1599 (2014).
33. F. N. Keutsch, J. D. Cruzan, R. J. Saykally, *Chem. Rev.* **103**, 2533 (2003).

34. B. Temelso, K. A. Archer, G. C. Shields, *J. Phys. Chem. A* **115**, 12034 (2011).
35. Y. Wang, V. Babin, J. M. Bowman, F. Paesani, *J. Am. Chem. Soc.* **134**, 11116 (2012).
36. V. Babin, F. Paesani, *Chem. Phys. Lett.* **580**, 1 (2013).
37. H. C. Longuet-Higgins, *Mol. Phys.* **6**, 445 (1963).
38. J. O. Richardson, S. C. Althorpe, *J. Chem. Phys.* **134**, 054109 (2011).
39. J. O. Richardson, *et al.*, *J. Phys. Chem. A* **117**, 6960 (2013).
40. S. Chapman, B. C. Garrett, W. H. Miller, *J. Chem. Phys.* **63**, 2710 (1975).
41. T. Mitsui, M. K. Rose, E. Fomin, D. F. Ogletree, M. Salmeron, *Science* **297**, 1850 (2002).
42. V. A. Ranea, *et al.*, *Phys. Rev. Lett.* **92**, 136104 (2004).
43. J. Nichols, H. Taylor, P. Schmidt, J. Simons, *J. Chem. Phys.* **92**, 340 (1990).
44. J.-Q. Sun, K. Ruedenberg, *J. Chem. Phys.* **99**, 5257 (1993).
45. R. P. Feynman, A. R. Hibbs, *Quantum Mechanics and Path Integrals* (McGraw-Hill, New York, 1965).
46. W. H. Miller, *J. Chem. Phys.* **55**, 3146 (1971).
47. A. I. Vainshtein, V. I. Zakharov, V. A. Novikov, M. A. Shifman, *Sov. Phys. Uspekhi* **25**, 195 (1982). Also in *Instantons in Gauge Theories*, edited by M. Shifman, pp. 468 (Singapore: World Scientific, 1994).
48. C. Zhu, R. H. Byrd, P. Lu, J. Nocedal, *ACM Trans. Math. Softw.* **23**, 550 (1997).

49. A. A. Reid, Quantum tunnelling splittings in water clusters, from ring-polymer instanton theory, Ph.D. thesis, University of Cambridge (2014).
50. T. R. Dyke, *J. Chem. Phys.* **66**, 492 (1977).
51. P. R. Bunker, P. Jensen, *Fundamentals of molecular symmetry* (Institute of Physics, 2005).
52. P. R. Bunker, P. Jensen, *Molecular Symmetry and Spectroscopy* (NRC Research Press, Ottawa, 2006), second edn.
53. G. T. Fraser, R. D. Suenram, L. H. Coudert, *J. Chem. Phys.* **90**, 6077 (1989).
54. N. A. Seifert, *et al.*, *J. Mol. Spectrosc.* **312**, 13 (2015).
55. W. Gordy, R. L. Cook, *Microwave Molecular Spectra*, in: W. West (Ed.), *Chemical Applications of Spectroscopy*, Part II, Vol. IX, (Wiley Interscience, New York, 1970).
56. G. G. Brown, *et al.*, *Rev. Sci. Instrum.* **79**, 053103 (2008).
57. Z. Kisiel, *J. Mol. Spectrosc.* **218**, 58 (2003).
58. D. F. Plusquellic, R. D. Suenram, B. Mat, J. O. Jensen, A. C. Samuels, *J. Chem. Phys.* **115**, 3057 (2001).
59. Z. Kisiel, *et al.*, *J. Mol. Spectrosc.* **233**, 231 (2005).
60. Z. Kisiel, *et al.*, *J. Mol. Spectrosc.* **280**, 134 (2012).
61. H. M. Pickett, *J. Mol. Spectrosc.* **148**, 371 (1991).
62. H. M. Pickett, SPFIT/SPCAT package, available at <http://spec.jpl.nasa.gov>

63. J. K. G. Watson, *Aspects of quartic and sextic centrifugal effects on rotational energy levels*, in: J. R. Durig (Ed.), *Vibrational Spectra and Structure*, vol. 6, (Elsevier, New York/Amsterdam, 1977), pp. 189.
64. Z. Kisiel, *Assignment and Analysis of Complex Rotational Spectra*, in J. Demaison *et al.* (Eds.), *Spectroscopy from Space*, (Kluwer Academic Publishers, Dordrecht, 2001).
65. Z. Kisiel, PROSPE – Programs for ROTational SPEctroscopy, available at www.ifpan.edu.pl/~kisiel/prospe.htm
66. E. F. Pettersen, *et al.*, *J. Comput. Chem.*, **13**, 1605 (2004).

* The authors acknowledge financial support from a European Union COFUND/Durham Junior Research Fellowship (JOR), a Research Fellowship from the Alexander von Humboldt Foundation (CP), the U.S. National Science Foundation grants CHE-0960074 (CP, BHP), CHE-1213521 and CHE-1229354 (BT, GCS), the Swiss National Science Foundation grant PBBEP2-144907 (SL), the UK Engineering and Physical Sciences Research Council (AAR, DJW, SCA), and a grant from the Polish National Science Centre, decision number DEC/2011/02/A/ST2/00298 (ZK).

Supplementary Materials

www.sciencemag.org

Materials and Methods

Figs. S1–S9

Tables S1–S74

References (43–66)

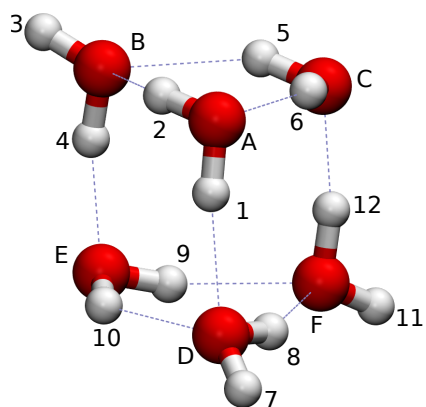


Figure 1: Minimum-energy structure of the PR1 prism isomer of the water hexamer. The labels define one version (i.e. arrangement of the atoms) which can tunnel to other versions by permuting identical atomic nuclei within the structure.

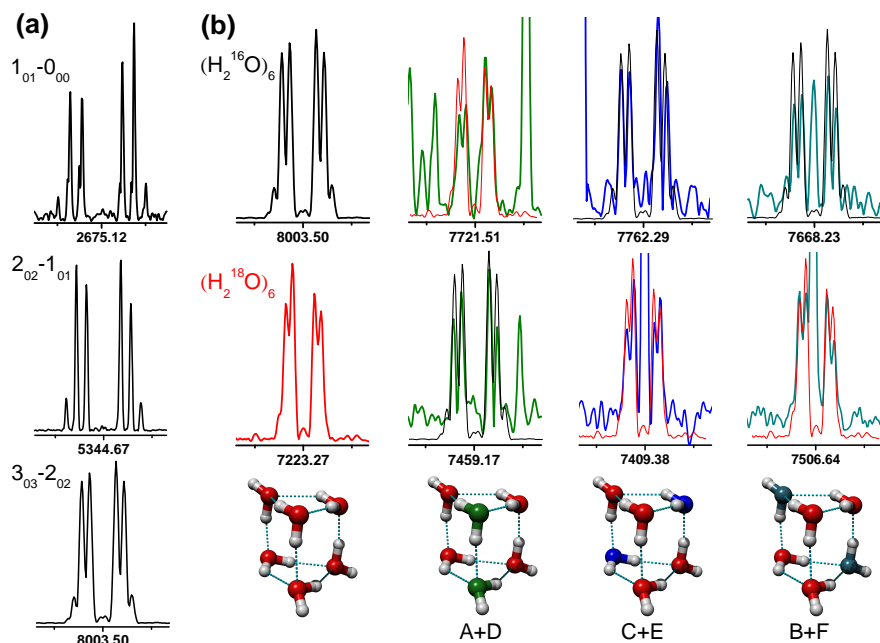


Figure 2: Rotational spectral evidence for tunneling. (a) Three spectra for the $(\text{H}_2^{16}\text{O})_6$ PR1 prism, showing the doublet-of-triplets splitting pattern attributed to tunneling. The rotational levels involved in each transition are denoted using the standard asymmetric top notation, $J_{K_a K_c}$. The labeled frequency is the asymmetric-top rotational transition-frequency and the tunneling pattern is symmetric around this frequency. (b) The $3_{03} - 2_{02}$ spectra for the 8 isotopologues (of 64 possible) that display tunneling. Tunneling is observed for both the $(\text{H}_2^{16}\text{O})_6$ transition centered at 8003.50 MHz (black trace) and the $(\text{H}_2^{18}\text{O})_6$ transition centered at 7223.27 MHz (red trace), and the width of the splitting pattern is reduced for the heavier isotopologue. The other isotopologues that show tunneling have either two H_2^{18}O substitutions in the $(\text{H}_2^{16}\text{O})_6$ structure (top row) or two H_2^{16}O substitutions in the $(\text{H}_2^{18}\text{O})_6$ cluster (bottom row). The substituted positions are depicted by the molecular structures at the bottom. All six of the doubly-substituted clusters have a tunneling splitting (green and blue traces) that matches either the $(\text{H}_2^{16}\text{O})_6$ or $(\text{H}_2^{18}\text{O})_6$ clusters as shown by the overlay of these spectra. All four spectra where water molecules A+D are H_2^{16}O have the same, larger splitting (black trace) while all four clusters where A+D are H_2^{18}O have the reduced tunneling splitting (red trace). The additional transitions observed in the doubly-substituted spectra come from rotational transitions of other water cluster isotopologues and are not part of the tunneling-splitting pattern. The tick marks in all panels have 1 MHz spacing.

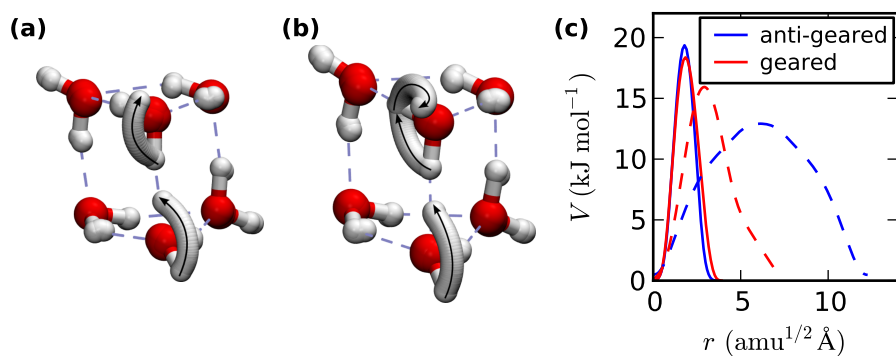


Figure 3: Instanton tunneling pathways in the water hexamer prism. (a) Anti-gearred and (b) geared variations. The pathways are shown as conflated snapshots of replicas of the system obtained from ring-polymer representations of the instantons. Note that the geared pathway involves the concerted breaking of two hydrogen bonds. (c) Variation of the potential energy along the instanton paths (solid lines) and minimum-energy paths (dashed lines), where r is the integrated mass-weighted path length, and V is the potential energy along the path.

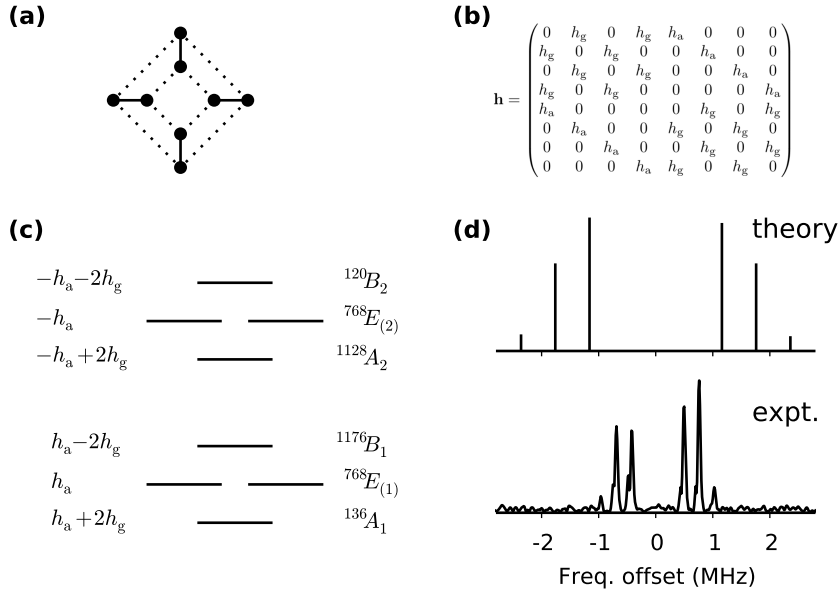


Figure 4: Origin of the splitting pattern. (a) Graph showing how the versions (vertices) are connected by the tunneling paths (lines: anti-g geared–solid, geared–dotted). Diagonalization of the associated tunneling matrix, \mathbf{h} , defined in (b) splits the ground-state energy level shown as shown in (c), where the symmetry is also given with its nuclear-spin degeneracy as a superscript. The states labeled $E_{(1)}$ and $E_{(2)}$ both have symmetry E . The rotational spectrum involves transitions between the tunneling level patterns for different rotational energy levels. The resulting tunneling-splitting pattern centered on the expected rotational transition frequency is: $2h_a + 4h_g$, $2h_a$, $2h_a - 4h_g$, $-2h_a + 4h_g$, $-2h_a$, $-2h_a - 4h_g$, where h_a and h_g are the average values of the anti-g geared and geared tunneling matrix elements in the rotational energy levels for the spectroscopic transition. This spectral pattern is plotted in (d) using the theoretical matrix elements as the average values in the rotational levels and is compared with the measured $1_{01} - 0_{00}$ transition (represented to scale). This explains the observed doublet-of-triplets splitting pattern where the outermost lines are considerably smaller.